

MODAL-BASED FUEL LEVEL ESTIMATION OF CRYOGENIC PROPELLANT TANKS

Simon Pfeifer[1], Fynn Thilker[1], Andreas Tramposch[1] & Armin Buchroithner[2]

[1]FH JOANNEUM, Institute of Aviation, Graz, Austria
[2]University of Technology, Institute of Electrical Measurement and Sensor Systems, Graz, Austria

Abstract

Hydrogen-powered aircraft are widely regarded as a key enabler for carbon-neutral aviation, yet their implementation introduces significant challenges, among them, problems related to cryogenic fuel storage and thermal management. In particular, reliable fill-level measurement in liquid hydrogen tanks remains difficult as extreme temperatures and two-phase flow behavior result in limitations of the application of conventional sensing technologies. This work investigates a non-invasive modal-based approach for fill-level estimation, using shifts in structural resonance frequencies caused by changes in contained liquid mass. mass. Fill level measurements via modal analysis are potentially robust against flight maneuvers leading to sloshing, while avoiding tank penetration and direct heat input. The approach combines experimental and numerical results obtained for the investigated fill levels and sensor configurations. A suspended $50\,\mathrm{l}$ steel pressure vessel was tested at five fill levels between 0 % and 100 %, using externally mounted acceleration sensors and shaker excitation. Water was used as a substitute fluid for a qualitative proof-of-concept study. The measured frequency response functions were analyzed with respect to fill-level-dependent frequency shifts and compared with simplified finite element models based on density variation and distributed added mass. The results show that selected resonance frequencies exhibit clear and trackable shifts with increasing fill level, confirming the basic feasibility of modal-based fill-level estimation. However, not all modes are equally suitable, and deviations between simulation and experiment increase for higher fill levels and fluid-influenced resonances. The study demonstrates the potential of modal gauging as a non-invasive measurement concept for cryogenic aircraft tank systems, while further work is required regarding repeatability, accuracy, and fluid-structure interaction effects under representative cryogenic conditions.

Keywords: Fuel gauging, cryogenic, liquid hydrogen storage, liquid nitrogen, modal analysis

1. Introduction

As the demand for clean aviation and emission reduction continues to increase, a wide range of alternative propulsion concepts is currently under investigation. Achieving global net-zero targets requires a transition away from conventional kerosene-based propulsion, as aircraft powered by fossil fuels represent a significant contributor to global CO_2 emissions [1]. Among the proposed alternatives, hydrogen-powered aircraft are considered a promising pathway toward decarbonizing the aviation sector [2].

Depending on the selected propulsion concept, hydrogen may be utilized either in fuel cells to generate electrical power or be directly combusted in gas turbines to produce thrust. These approaches differ in efficiency and technological maturity [3, 4]. However, in both cases hydrogen storage introduces significant technical challenges, as the chosen physical state strongly affects system design and operation [5]. While gaseous hydrogen is typically stored at pressures of up to $700\,\mathrm{bar}$, liquid hydrogen (LH_2) offers a substantially higher gravimetric energy density and approximately three times the specific energy per unit mass compared to conventional jet kerosene. Consequently, LH_2 is widely

regarded as the preferred storage option for aviation applications. However, its storage at cryogenic temperatures below $20\,\mathrm{K}$ introduces considerable challenges related to thermal management, boil-off control, and system integration [6, 7].

State of the Art

Reliable fuel management is also of critical importance, requiring robust and accurate fill-level measurement techniques. Common techniques, typically used in civil aircraft for wing embedded tank systems, such as capacitance probes, ultrasonic sensors, or float gauges rely on warm, stable fluids and well-defined interfaces, assumptions that are not applicable in cryogenic conditions, particularly during dynamic operation [8, 9]. Hence, these conventional sensing approaches are significantly affected by the cryogenic environment, including low temperatures, low fluid densities, and two-phase flow behavior [1, 10]. Furthermore, according to recent studies, such as [11], the structure and layout of LH_2 tank systems need to be significantly adapted compared to kerosene tank systems and tend to be placed in the fuselage with a cylindrical design, due to pressure induced increased structural stiffness requirements, safety reasons and practicability. As a consequence, the transferability of existing concepts is further limited.

Additional challenges arise from vapor and ice formation, in case of water retention, on moving or optical components, and degradation of material properties at cryogenic temperatures as well as hydrogen embrittlement of certain materials further limiting the applicability of traditional methods [12]. Despite extensive research into cryogenic level measurement methods such as thermal, hydrostatic, superconducting, diode-based, and optical techniques, either significant limitations persist or the technologies have not yet attained sufficient maturity for aerospace cryogenic tank applications [8, 13, 14, 15, 16, 17].

As an alternative, modal or eigenfrequency-based gauging has gained increasing attention, particularly in space applications under microgravity conditions. This approach exploits the dependence of a tank's structural or acoustic eigenfrequencies on the mass of the contained liquid. Variations in fill level induce measurable eigenfrequency shifts that can be tracked via the tank's frequency response function using externally mounted accelerometers or piezoelectric actuators. Because the method senses global fluid mass rather than local fluid motion, it is inherently non-invasive and robust to sloshing effects, enabling reliable measurements even under dynamic conditions [18, 19]. While most studies have focused on microgravity environments, the underlying physical principle remains valid under terrestrial gravity. Experimental investigations have demonstrated the applicability of modal gauging in settled $1\,\mathrm{g}$ tanks, achieving measurement accuracies on the order of $1.5\,\%$ to $2\,\%$ of the total tank volume [20].

Although modal propellant gauging has already been investigated, particularly for space and reduced-gravity applications, its transferability to aircraft-related cryogenic tank systems remains insufficiently established. In particular, the influence of structural tank dynamics, sensor placement, and simplified numerical mass-loading approaches on the practical applicability of modal-based fill-level estimation requires further investigation.

In this work, modal-based fill-level estimation is applied to terrestrial cryogenic propulsion tanks as part of a broader research effort on cryogenic composite tank technologies. The use of non-invasive measurement techniques is particularly important to preserve the structural integrity and mechanical performance of carbon-fiber-reinforced materials, as tank penetration or embedded sensors would complicate maintenance, repair and thermal bridges would be established, which will increase the heat transfer, thus raising the boil-off rate and consequently loosing costly fuel, if the boil-off gas can not be recovered and used for combustion [21]. The main contribution of this work is the application-oriented assessment of modal-based fill-level estimation for aircraft-related cryogenic tank systems. Beyond demonstrating the general principle, the study evaluates mode selection, sensor-position dependency, and the limitations of simplified added-mass models for predicting experimentally observed fill-level-dependent frequency shifts. The basic suitability of modal-based fill-level detection is

investigated under simplified boundary conditions in this paper by experimental modal investigation at five fill levels and identifying fill-sensitive eigenmodes. The focus lies on the relative variation of modal characteristics with changing fill level rather than the exact quantitative determination of absolute eigenfrequencies. Furthermore, a comparative approach was initiated to assess the correlation between various simulation methods and the experimental study.
However, in Figure 1 a flowchart schematics of the experimental setup can be seen, including the tank, exciter, accelerometer and signal processing in a general overview.

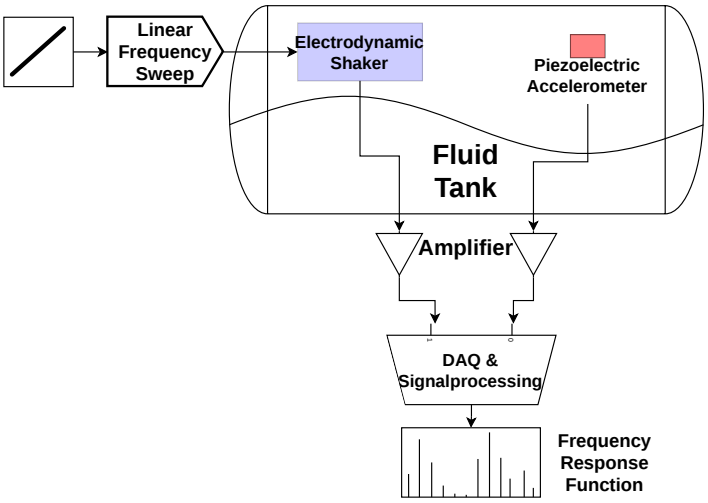


Figure 1 – Schematics of the Experimental Setup

2. Theoretical Background

The dynamic behavior of mechanical systems, thus natural frequencies, damping ratios, and mode shapes can be described by modal analysis. For linear elastic structures, the vibration response can be represented as a superposition of individual eigenmodes, each corresponding to a specific resonance frequency and deformation pattern of the structure [22].
Since the focus of this work lies on the relative shift of natural frequencies rather than on the quantitative prediction of resonance amplitudes or damping behavior, the basic modal formulation is introduced using the undamped equation of motion, which is given by

$$\mathbf{M}\ddot{\mathbf{x}} + \mathbf{K}\mathbf{x} = 0 \tag{1}$$

where $\mathbf{M}$ denotes the mass matrix, $\mathbf{K}$ indicates the stiffness matrix, and $\mathbf{x}$ is defined as the displacement vector. Assuming harmonic motion,

$$\mathbf{x}(t) = \phi e^{i\omega t} \tag{2}$$

leads to the classical eigenvalue problem

$$\left(\mathbf{K} - \omega^2 \mathbf{M}\right)\phi = 0 \tag{3}$$

with eigenfrequencies ω and corresponding eigenvectors ϕ representing the mode shapes [23].
For fluid-filled tanks, the dynamic system is additionally influenced by the fluid mass and fluid-structure interaction effects. An increase in fill level changes the effective system mass and therefore has an impact on the natural frequencies of the system. In general, increasing mass leads to a reduction of the eigenfrequencies according to

$$\omega_n \propto \sqrt{\frac{k}{m}} \tag{4}$$

where k represents the effective stiffness and m the effective modal mass. The solution of the eigenvalue problem yields the angular natural frequencies ω_n. For improved interpretability and direct comparison with the experimental results, the natural frequencies are expressed in Hertz according to

$$f_n = \frac{\omega_n}{2\pi}. \tag{5}$$

Besides structural modes, additional fluid-dominated or coupled fluid-structure modes may occur depending on the fill level and fluid behavior [24, 25]. In addition to mass variations, the modal characteristics of thin-walled tanks are also affected by changes in internal pressure. Pressure fluctuations arising from evaporation, pressurization processes, sloshing, or filling and draining operations alter the effective stiffness of the tank walls and can therefore influence the natural frequencies, particularly of lower-order structural modes. As pressure-induced stiffness increases generally lead to higher natural frequencies, their effect may partially offset the frequency reduction caused by increasing fluid mass [18, 26].
In simplified numerical approaches, the fluid influence can be represented by an added-mass formulation. Pressure-based acoustic fluid formulations, in contrast, can account for acoustic pressure fields and coupled structural-acoustic modes, but remain based on a linearized fluid representation. Such models require a more detailed definition of the fluid domain, interface coupling, boundary conditions, and material properties, and generally involve higher computational effort. Moreover, acoustic formulations do not inherently capture nonlinear free-surface motion or large-amplitude sloshing [24, 25]. The added-mass formulation was therefore used as a first-order approximation to isolate the inertial effect of the fluid mass and to provide a computationally efficient reference model. More detailed acoustic or coupled fluid-structure-interaction models are considered necessary for future work where pressure fields, coupled resonances, and free-surface effects are investigated explicitly. The distinction between structural and fluid-dominated modes is therefore essential for modal-based fill level estimation.

The dynamic response of a system can be evaluated using the Frequency Response Function (FRF), which describes the relationship between the excitation input and the measured structural response in the frequency domain. The FRF is commonly expressed as

$$H(\omega) = \frac{X(\omega)}{F(\omega)} \tag{6}$$

where $X(\omega)$ denotes the response spectrum and $F(\omega)$ the excitation spectrum. Resonance frequencies appear as peaks in the FRF and allow the identification of modal properties such as eigenfrequencies and damping characteristics [22].

Sampling Criteria

Since the experimental identification of these resonance peaks relies on digitally acquired time-domain signals, the sampling parameters must be selected such that the relevant frequency content is captured without distortion. In order to avoid aliasing effects for digital signal acquisition, the sampling frequency of the measured signal must satisfy the Nyquist criterion. The Nyquist frequency, f_{Nyquist}, is defined as half of the sampling frequency,

$$f_{\text{Nyquist}} = \frac{f_s}{2} \tag{7}$$

where f_s is the sampling frequency. Only frequency components below the Nyquist frequency can be reconstructed correctly from sampled data [22]. Therefore, the sampling frequency used in modal testing must be selected sufficiently high to capture all relevant structural and fluid-related resonances.

Mass Ratio Considerations for Modal Fill-Level Estimation

Furthermore, beyond the measurement requirements, the sensitivity of modal-based fill-level estimation is governed by the physical mass distribution of the tank system and is important for the selection of the experimental setup. Since the effective system mass is a key parameter governing the natural frequencies of a structure, the ratio between the tank dry mass m_{tank} and the fuel mass m_{fuel} directly influences the sensitivity and significance of modal-based fill-level estimation.

Gomez et al. [27] and Onorato et al. [28] characterize the structural efficiency of an aircraft fuel storage system using the tank-to-fuel mass ratio

$$\lambda = \frac{m_{\text{tank}}}{m_{\text{fuel}}}, \tag{8}$$

which quantifies the amount of tank mass required per unit mass of stored fuel. However, a complementary metric frequently used in hydrogen storage literature, including the work of Huete et al. [29], is the gravimetric efficiency

$$\eta_{\text{grav}} = \frac{m_{\text{fuel}}}{m_{\text{fuel}} + m_{\text{tank}}}, \tag{9}$$

which represents the fraction of the total storage system mass that consists of usable fuel. Both quantities are directly related through

$$\eta_{\text{grav}} = \frac{1}{1+\lambda}. \tag{10}$$

In conventional aircraft, kerosene is typically stored integrally within the wing structure in a so-called wet-wing configuration, eliminating the need for dedicated pressure vessels and resulting in very low tank structural mass fractions [30]. Typical values are in the range of $\lambda \approx 0.03$–0.06, corresponding to gravimetric efficiencies above $94\,\%$. In contrast, cryogenic LH_2 storage systems generally exhibit significantly higher tank mass fractions due to insulation, pressure containment, and structural requirements. Gomez et al. [27] and Onorato et al. [28] report optimistic estimates of $\lambda \approx 0.2$–0.45. However, Huete et al. [31] present a more conservative assessment, suggesting values in the range of $\lambda \approx 0.4$–1.3. These estimates provide a baseline for obtaining a suitable and transferable ratio of structural to fluid mass for the experimental setup, which is approximately $\lambda \approx 0.5$ in the present experimental setup.

3. Methods

The methodology combines numerical modal analysis and experimental investigations to evaluate the feasibility of non-invasive fill-level estimation based on eigenfrequency shifts caused by mass variations. A finite element model of the tank was developed in Ansys Workbench to investigate the influence of increasing fluid mass on the dynamic behavior, thus the natural frequencies and mode shapes of the system. Different simulation approaches and discrete fill levels were considered to evaluate the capability of the numerical models to reproduce the experimentally observed modal behavior.

The numerical studies were used to identify the relevant frequency range of interest for the experimental measurements, estimate mode shapes for selecting suitable sensor locations, and support the design of the experimental investigations. Key parameters such as fill level, gravity orientation, and boundary conditions were considered in order to assess their influence on the modal characteristics of the tank. Furthermore, the material properties and geometric characteristics of the structure were incorporated into the numerical model to enable a direct comparison with the experimental results. The simulation results were subsequently compared with the measured frequency response functions to assess the applicability of simplified mass-loading models for modal-based fill-level estimation.

3.1 Experimental Setup

For the experimental investigations, a commercially available galvanized steel pressure vessel manufactured by MABE with a total volume of $50\,\text{l}$ was used. The tank is designed for a maximum operating

pressure of $16\,\mathrm{bar}$ and consists of a cylindrical shell structure with hemispherical end caps. The wall thickness is $3.5\,\mathrm{mm}$, while the total mass of the empty tank, including all plugs and permanently mounted support feet, is $25.3\,\mathrm{kg}$.
A full-scale cryogenic tank was not used at this stage, since aircraft-relevant cryogenic tanks require a more complex double-walled and vacuum-insulated architecture to limit heat ingress and boil-off losses. Such systems are associated with significantly higher costs, and additional thermal, structural, and safety-related design constraints. The present tank was therefore selected as a simplified laboratory-scale demonstrator, allowing the fundamental influence of fluid mass on the modal response to be investigated under controlled conditions. Furthermore, tank was chosen to achieve a comparatively representative structural-to-fluid mass ratio for laboratory-scale investigations of approximately $\lambda \approx 0.5$, similar to estimations of aircraft $\mathrm{LH_2}$ tank systems, corresponding to a maximum fluid mass of approximately $50\,\mathrm{kg}$ and a total system mass of approximately $75\,\mathrm{kg}$ at full fill level.

Due to safety considerations and simplified handling procedures, experiments with cryogenic fluids were not conducted within the scope of this study. Instead, water was used as a substitute fluid for $\mathrm{LH_2}$ for qualitative proof-of-concept.
To minimize the influence of external boundary conditions and avoid undesired mechanical constraints, the tank was string suspended with a priority on minimizing vibrations by using multiple elastic expanders attached to the tank feet, which can be seen in Figure 2a. This suspension configuration was selected to approximate free-free boundary conditions and to allow unrestricted structural vibration behavior over a broad frequency range. Additionally, it was designed such that its dominant dynamic influence remained below the primary frequency range of interest.

System excitation was introduced using a TIRA TV 50018 electrodynamic shaker. Due to the comparatively low nominal excitation force of the shaker and the lack of alternative excitation systems, the shaker was mounted directly onto the tank, which is visible in Figure 2b, in order to enhance force transmission into the structure and to improve vibrational energy transfer. For this purpose, a custom-fitted additively manufactured adapter in combination with a tension strap was used. The adapter was fabricated from Nylon PA12 reinforced with carbon fibers (PA12+CF15), selected for its comparatively high stiffness to ensure efficient transmission of excitation forces and reduce additional structural damping effects introduced by the mounting interface.
The direct shaker attachment may locally influence the structural dynamics due to additional mass and stiffness contributions. However, this configuration was necessary to achieve sufficient excitation amplitudes within the investigated frequency range. Furthermore, the influence of the shaker remains constant throughout all measurements and therefore only has a limited effect on the comparative analysis of the fill-level dependent modal behavior.

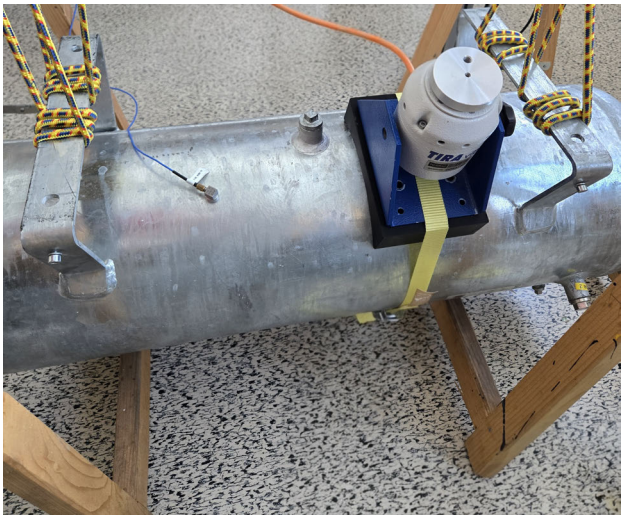
The structure was excited using a linear frequency sweep with a sweep duration of $20\,\mathrm{s}$, a center frequency of $1225\,\mathrm{Hz}$, a frequency span of $2150\,\mathrm{Hz}$, and an excitation amplitude of $5\,\mathrm{V}$. Furthermore, the shaker was intentionally positioned outside the principal symmetry and rotational axes of the tank in order to achieve broader modal excitation and reduce the risk of selectively suppressing specific vibration modes.

Five fill levels between $0\,\%$ and $100\,\%$ of the maximum fluid mass with increments of $25\,\%$ were experimentally investigated with respect to their modal characteristics. Structural vibrations of the tank wall were measured using a PCB Piezotronics accelerometer (model 333B30), which was attached to the external tank surface using a magnetic mounting base. The accelerometer converts mechanical vibrations into electrical signals, which were subsequently amplified and acquired using a PicoScope 5000 Series oscilloscope manufactured by Pico Technology. Signal acquisition and processing were performed using the PicoScope 7 software environment, while the analysis was carried out with MATLAB.

Measurements were conducted at four different sensor locations distributed across the tank surface.



(a) Experimental setup using string suspension (modified using AI-based image processing)



(b) Accelerometer and Shaker on the vessel

Figure 2 – Experimental Setup

Sensor placement, which can be found in Figure 3, was selected such that potential nodal regions were avoided as far as possible, based on prior numerical simulation results and preliminary experimental observations. While sensor position 1 was chosen to be next to the shaker, position 4 was approximately on the opposite side. Furthermore, the numerical investigations indicated that resonance phenomena within the frequency range between approximately 150 and $2500\,\mathrm{Hz}$ are particularly relevant for fill-level dependent modal behavior. Consequently, the sampling frequency of the analog-to-digital converter was set to $f_s = 20\,\mathrm{kSamples/s}$, thereby satisfying the Nyquist criterion according to equation (7)

$$f_s > 2 \cdot f_{\max} \tag{11}$$

with $f_{\max} = 2500\,\mathrm{Hz}$.

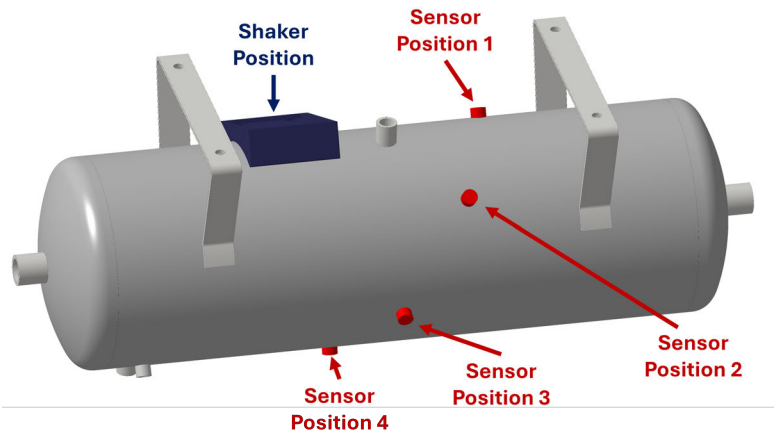


Figure 3 – Positioning of sensor and shaker placement

3.2 Simulation Models

To investigate the influence of varying fill levels on the modal behavior of the tank system, numerical modal analyses were performed in Ansys Modal Analysis embedded in Ansys Workbench. The objective of the simulations was not only to approximate the experimentally observed natural frequencies, but also to assess how far simplified mass-based models can represent the fill-level dependent

dynamic behavior. Two different added-mass approaches were investigated, each for the same five fill levels as used in the experimental measurements. Both approaches neglect acoustic effects, liquid pressure fields, and the dynamic behavior of the fluid, and therefore represent only the inertial influence of the added liquid mass.

3.2.1 Material Model and Simplifications

The original CAD geometry from the manufacturer resulted in an overprediction of the structural mass with an assumption of a material density of $7850\,\mathrm{kg/m^3}$ for standard structural steel, which was chosen from a material data base, as the material was not further characterized by the manufacturer. Therefore, the wall thickness was adjusted from $5\,\mathrm{mm}$ to $3.5\,\mathrm{mm}$ such that the FE model matched the experimentally measured tank mass of $25\,\mathrm{kg}$. The Young's Modulus for structural steel, derived from the data base, is defined with $200\,\mathrm{GPa}$, while the Poisson's Ratio is specified with 0.3. Furthermore, the influence of the weight of the shaker and the piezoelectric sensor were neglected and not included in the model. Additionally, free–free boundary conditions were applied in the simulations in order to approximate the experimental suspension setup. This suspension method is commonly used to approximate unconstrained conditions by shifting the suspension modes to frequencies significantly lower than the structural eigenfrequencies of interest. Consequently, no additional supports or constraints were applied in the finite element model, and the first six rigid-body modes were excluded from the evaluation.

In order to reduce model complexity and computational effort, the following simplifications were introduced in the numerical model:

- Weld seams
- local variations in sheet thickness
- detailed contact interactions between structural components
- residual fluid quantities
- inherent material damping

These simplifications may partly explain deviations between the numerical predictions and the experimentally observed modal characteristics.

3.2.2 Different Approaches

As a baseline case, a purely structural finite element model of the empty tank was created. The model was based on the provided CAD geometry of the manufacturer of the pressure vessel, including the main tank body as well as the relevant fittings and connections. The investigated tank has a nominal volume of $50\,\mathrm{l}$, with an internal diameter of approximately $269\,\mathrm{mm}$ and with $3.5\,\mathrm{mm}$ sheet thickness, an overall length of approximately $900\,\mathrm{mm}$, and hemispherical end caps. This model serves as a reference state for the identification of the fundamental shell and structural modes of the tank without any fluid interaction effects. It allows the investigation of the intrinsic dynamic characteristics of the tank geometry and material properties and provides an initial estimation of the dominant resonance frequencies.

As an alternative methodology to fluid-structure interaction analysis, the influence of the fluid, which is water, was approximated using an added mass formulation. In this simplified representation, the fluid contribution is modeled as an additional inertial load acting on the structure. This approach captures the general reduction of eigenfrequencies caused by increasing effective system mass at higher fill levels. However, since the fluid itself is not modeled as a dynamic domain, fluid dominated resonances and coupled fluid-structure modes cannot be represented using this method. Consequently, nonlinear free-surface effects and sloshing phenomena are also not captured within the scope of the

present simulations.

In the first approach, the density of the structural material was increased such that the total mass of the model corresponded to the combined mass of the tank structure and the contained liquid. This results in a homogenized distribution of the additional mass over the entire tank structure. In the second approach, the additional liquid mass was applied as a distributed mass on the inner wall of the tank using the distributed mass functionality in Ansys Mechanical. This approach introduces the additional inertia more locally at the fluid-contacting surface, while still not representing the fluid as a dynamic domain.

For the empty tank and the added mass configuration, an undamped modal analysis was conducted. The modal analyses were performed using the direct solver in combination with the Block Lanczos eigensolver.

3.2.3 Mesh Convergence study

A mesh convergence study was conducted in order to assess the sensitivity of the numerical results with respect to the spatial discretization. Four different element sizes were evaluated, ranging from $15\,\mathrm{mm}$, $7.5\,\mathrm{mm}$, $3.5\,\mathrm{mm}$ down to $1.5\,\mathrm{mm}$, resulting in meshes with just over 3 million elements for the finest configuration. Quadratic element order was used throughout the study to improve the accuracy of the displacement field representation, particularly for capturing curved geometries and higher-order structural modes. A sweepable meshing strategy was applied where possible, in order to ensure a structured element alignment through the thickness of the shell regions, which is beneficial for accurately resolving bending dominated behavior in thin-walled structures.

The mesh was generated using tetrahedral elements, which provide a robust and flexible discretization approach for complex geometries such as cylindrical shells with hemispherical end caps and local geometric details.
The results of the convergence study showed only a minor variation in the identified eigenfrequencies with mesh refinement. The influence of mesh refinement on the calculated eigenfrequencies was evaluated by comparing selected resonance modes. For example, one representative mode was obtained at approximately $334\,\mathrm{Hz}$ using an element size of $15\,\mathrm{mm}$, while the same mode converged towards $327\,\mathrm{Hz}$ for $3.5\,\mathrm{mm}$ and approximately $324\,\mathrm{Hz}$ for the finest mesh with $1.5\,\mathrm{mm}$ element size, in order to have at least two layers within the tank's thickness. Since the relative deviation between the finer meshes becomes comparatively small while the computational effort increases significantly, a medium mesh size of approximately $3.5\,\mathrm{mm}$ was selected for the subsequent simulations as a compromise between numerical accuracy and computational cost.

4. Results

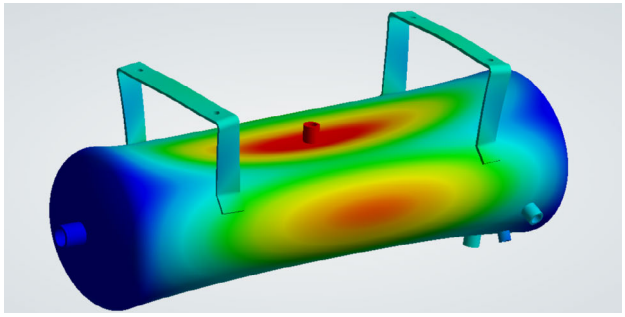
This section presents the experimental and numerical results obtained for the investigated fill levels and sensor configurations. The measured modal responses are analyzed with respect to fill-level dependent frequency shifts, resonance behavior, and the occurrence of possible fluid-structure interaction effects. Furthermore, the experimental observations are compared with the different numerical modeling approaches in order to evaluate their capability to reproduce the observed modal characteristics and to distinguish between structural and fluid-dominated resonances.

4.1 Simulation Comparison

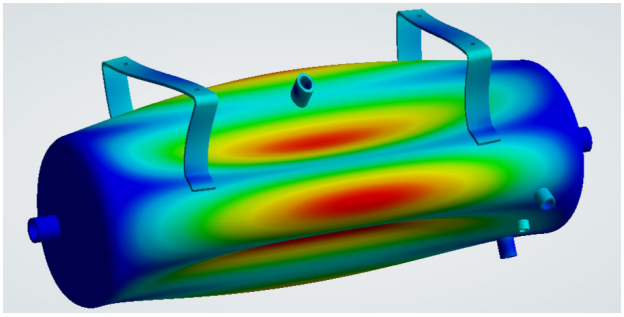
For both simulation approaches, the first 30 natural frequencies and corresponding mode shapes were calculated in order to identify the relevant frequency range for the experimental investigations and to obtain an initial estimate of the expected modal behavior. The first six modes, located between approximately $0\,\mathrm{Hz}$ and $2 \times 10^{-3}\,\mathrm{Hz}$, were excluded from the evaluation, as they correspond to rigid body modes resulting from the applied free-free boundary conditions. In addition, modes primarily

associated with the support feet were neglected, since the focus of this study lies on the modal behavior of the tank structure itself.

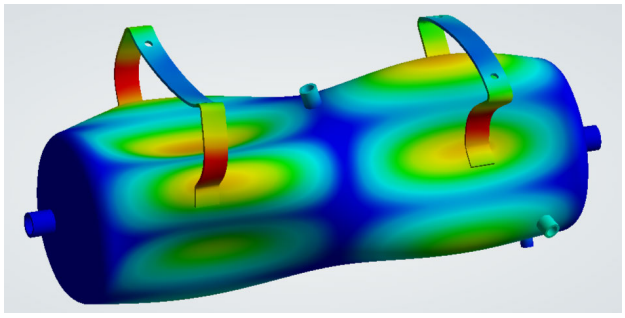
The structural modes of the tank show circumferential nodal patterns and, for higher-order modes, additional nodal lines in the axial direction, as shown in Figure 4 for selected empty-tank mode shapes. The first two depicted shell dominated modes, depicted in Figure 4a at approximately $330\,\mathrm{Hz}$ and in Figure 4b at approximately $396\,\mathrm{Hz}$, exhibit two and three circumferential nodal patterns, respectively, with the largest displacements occurring near the center of the cylindrical section. Nonetheless, the mode shown in Figure 4c at approximately $657\,\mathrm{Hz}$ represents a higher-order shell mode with nodal patterns in both the axial and circumferential directions.



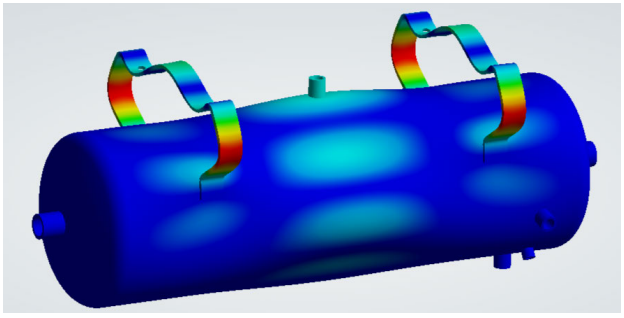
(a) First shell mode at $330\,\mathrm{Hz}$



(b) Third shell mode at $396\,\mathrm{Hz}$



(c) Sixth shell mode at $657\,\mathrm{Hz}$



(d) Twelfth shell mode at $910\,\mathrm{Hz}$

Figure 4 – Mode shape results of the tank at 0 % fill level

The displacement and mode shape of Figure 4d at $910\,\mathrm{Hz}$ was categorized as a support foot dominated eigenmode and was therefore not included in the statistical evaluation. However, as a matter of fact, this mode also exhibits three axial displacement nodes.

Both approaches essentially adhere to the same general trend, as can be seen in Figure 5. The tank fill level is shown on the y-axis, while the corresponding natural frequency is plotted on the x-axis. The solid lines with circular markers represent the density-variation approach, whereas the dashed lines with square markers correspond the alternative method using the distributed added mass approach.

It can be observed that the natural frequency curves obtained from the density-variation approach remain parallel for the different modes. This indicates a similar relative frequency reduction with increasing fill level. In contrast, the distributed added-mass approach leads to slightly different mode-dependent behavior, as the additional mass is applied locally to the inner tank wall rather than being homogenously distributed throughout the structure.
Furthermore, the frequency shift of a given mode is not linear over the investigated fill-level range. The relative change in natural frequency is more pronounced at lower fill levels and decreases as the fill level increases. A similar trend was also observed in the experimental results.

The empty tank modes have the same initial value for the different approaches, since, reasonably, no additional mass is present at a 0 % fill level. Consequently, there is no deviation in the results, as the

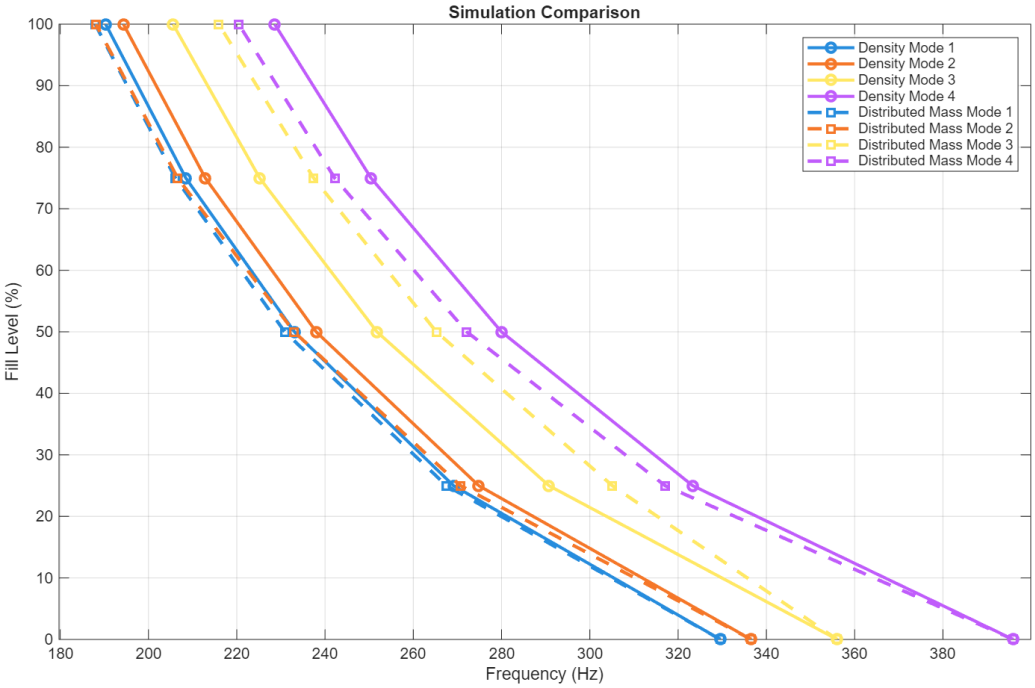


Figure 5 – Comparison of simulation methods
(variation in density vs. addition of a distributed mass)

simulations are identical. As the fill level increases, the relative difference of the eigenfrequency of each mode for both approaches also increases. The correspondence between individual modes was determined based on a comparison of their respective mode shapes.

Based on the simulation results, the accelerometer positions, which were shown beforehand in Figure 3, were chosen to avoid predicted nodal regions as far as possible and to ensure sufficient modal observability for various modes. In addition, the simulations were used to estimate the relevant frequency ranges for the experimental investigations.

4.2 Experimental Modal Response

The measured frequency response functions exhibit several dominant resonances within the investigated frequency range. While some modes remain relatively stable across all fill levels, other resonances show a clear shift in frequency and amplitude as the fluid mass increases. These observations indicate, as expected, a strong dependence of selected dynamic characteristics on the fill state of the tank.

A subset of identified modes is already present in the empty tank configuration and shows a gradual decrease in natural frequency with increasing fill level, which is consistent with added mass effects. In contrast, other resonances are significantly more sensitive to the presence of fluid and either emerge only at higher fill levels or exhibit a patternless frequency shift behavior. These modes are likely influenced by coupled fluid-structure interaction effects.
The observed frequency shifts are consistent across multiple measurement positions, indicating that the identified trends are not artifacts of local sensor placement but represent global changes in the dynamic behavior of the system.

Figure 6 shows the frequency response functions $|H(f)|$ measured at sensor position 4 for all five fill levels within a selected frequency range between $200\,\mathrm{Hz}$ and $400\,\mathrm{Hz}$, as this frequency window contains an identifiable and trackable resonance peak for all investigated fill levels. A clear shift of the resonance peak can be observed for each fill level. As expected, the fully filled tank exhibits the lowest resonance frequency, with a peak at approximately $215\,\mathrm{Hz}$, whereas the empty tank shows the corresponding peak at approximately $337\,\mathrm{Hz}$. This results in a frequency difference of $122\,\mathrm{Hz}$ between

the empty and fully filled configurations. Another notable characteristic is that the frequency spacing between adjacent fill-level peaks increases as the fill level decreases. This confirms a nonlinear relationship between the resonance frequency and the changing fluid mass.

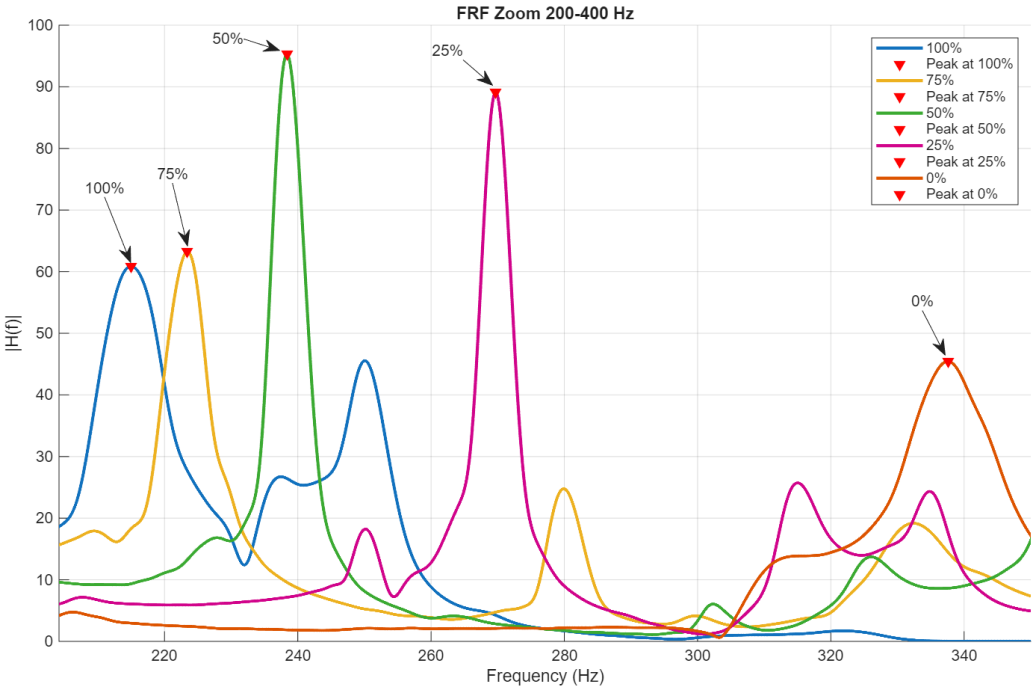


Figure 6 – FRFs of sensor position 4 for all five fill levels

Since the frequency spacing between the resonance peaks at 25 % and 0 % fill level is almost nine times larger than the spacing observed at higher fill levels ($68\,\mathrm{Hz}$ compared to approximately $8\,\mathrm{Hz}$), the resonance response appears to provide a higher distinguishability at lower fill levels. This suggests that the achievable fill-level resolution may not be constant over the entire filling range, but could improve as the fill level decreases, based on the observed resonance peak separation.

At sensor position 3 a resonance response at approximately $1000\,\mathrm{Hz}$ can be interpreted as a predominantly structural mode of the system. A corresponding peak is visible for all investigated fill levels, but its frequency shift does not follow a distinct fill-level dependent pattern. The highest response amplitude is observed for the empty tank, whereas the corresponding peaks for the filled configurations are considerably less pronounced while being located in the same frequency range.

A similar behavior is shown in Figure 7, which presents the frequency response functions measured at sensor position 1. A resonance peak around $1100\,\mathrm{Hz}$ can be observed for each fill level. However, no clear or consistent frequency shift pattern is visible. Therefore, this frequency range at this sensor position are not suitable for reliable fill-level estimation based on the present measurements.

Additionally, pronounced resonance peaks were observed at 50 % fill level at approximately $238\,\mathrm{Hz}$, $357\,\mathrm{Hz}$, and $541\,\mathrm{Hz}$. Since these peaks are significantly more pronounced than for the other fill configurations, they may indicate increased interaction between structural vibration modes and the fluid domain at this specific fill level.
However, a purely acoustic interpretation seems improbable. Estimating the acoustic wavelengths using $\lambda = c/f$ with a speed of sound in water of approximately $c = 1480\,\mathrm{m/s}$ results in wavelengths of approximately $6.2\,\mathrm{m}$, $4.1\,\mathrm{m}$, and $2.7\,\mathrm{m}$ for the three observed resonances. These values are significantly larger than the tank diameter of approximately $0.3\,\mathrm{m}$, suggesting that the resonances are unlikely to represent pure acoustic standing waves across the tank width. Since weak corresponding peaks are already present in the empty tank configuration, a purely fluid-dominated interpretation is

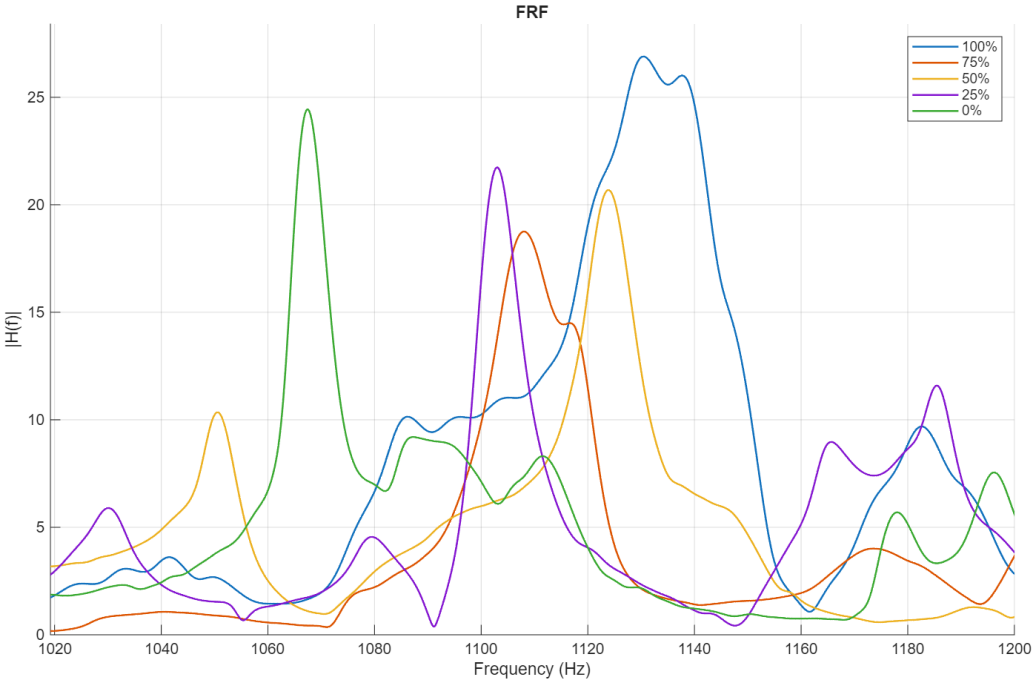


Figure 7 – FRFs at sensor position 1 show no distinct fill-level dependent pattern

also unlikely. Instead, the resonances are more plausibly associated with structural modes whose dynamic response is amplified or modified by the presence of the fluid. The observed behavior therefore suggests fluid-loaded structural modes or weakly coupled fluid-structure effects.

4.3 Fill-Level Sensitivity

To provide a simple reference for the experimentally observed frequency shifts, a single-degree-of-freedom approximation was used. For a given mode, the natural frequency can be expressed as

$$f_n = \frac{1}{2\pi}\sqrt{\frac{k_{\text{eff}}}{m_{\text{eff}}}}, \tag{12}$$

where k_{eff} and m_{eff} denote the effective modal stiffness and mass, respectively. Assuming that the structural stiffness remains approximately constant over the investigated fill levels, the frequency reduction can be estimated from the increase in effective mass.
Using the empty tank condition as reference, the normalized frequency shift is approximated by

$$\frac{f(\alpha)}{f_0} = \sqrt{\frac{m_0}{m_0 + \eta_m m_f(\alpha)}}, \tag{13}$$

Where f_0 is the resonance frequency of the empty tank, m_0 is the structural mass, $m_f(\alpha)$ is the fluid mass at fill level α, and η_m is an effective modal mass participation factor.
It should be noted that η_m does not represent a physical mass participation factor in the strict modal analysis sense. Instead, it serves as an effective parameter that quantifies the extent to which the experimentally observed frequency shift can be explained by a simplified added-mass approximation. The parameter can be interpreted as an effective measure of how strongly a particular mode is influenced by the presence of the fluid. In the simplest case, $\eta_m = 1$ corresponds to the assumption that the entire fluid mass contributes to the dynamic response. Values below unity indicate that only a fraction of the fluid mass participates in the considered mode.
This approximation is not intended to represent the full fluid-structure interaction behavior of the tank. Instead, it provides a reference trend for identifying modes whose frequency shift is mainly governed by added mass effects. Deviations from this trend may indicate additional effects such as

fluid-structure coupling, changes in modal stiffness, or fluid dominated resonances.

In Table 1, the eigenfrequencies of the experimental measurement of sensor position 4 and the results of eigenmode 2 using the variational density approach are displayed for all fill levels. As a baseline for the analytical calculation, f_0 was assumed to be $337\,\mathrm{Hz}$ at 0 % fill level, as the simulation and three of four sensor measurements were in this range. Within this table, the analytically predicted eigenfrequencies $f_{\mathrm{Prediction}}(\alpha)$ for all fill levels, except for the empty tank case were calculated using equation (13), while the effective modal fluid mass participation factor was assumed to be $\eta_m = 1$. The calculated natural frequencies match the simulated ones almost entirely, while the relative deviation from the experimental values is at a maximum of 10 % for the fully filled tank case. However, at fill level 50 % the measurement almost correspond the simulated and calculated value.
The observed deviations can be attributed to the simplified assumption of constant effective stiffness and to additional fluid induced effects that are not represented by this approximation.

Moreover, the effective modal fluid mass participation factor η_m was calculated from the experimental results listed in Table 1 using

$$\eta_m = \frac{m_0}{m_f(\alpha)} \left[\left(\frac{f_0}{f(\alpha)} \right)^2 - 1 \right], \tag{14}$$

which is a transformed version of Equation (13). Interestingly, at 25 % fill level, η_m is greater than 1. A literal interpretation of this value would imply that more than the entire added fluid mass contributes to the modal response, which is not physically meaningful. However, the measured frequency has decreased more than can be explained by the additional fluid mass using the simple added mass model. Values of η_m greater than unity indicate that the observed frequency reduction is larger than predicted by a simple added mass approximation. This suggests that the modal behavior cannot be explained by a pure increase in effective mass alone. Possible reasons include changes in effective modal stiffness or fluid-structure coupling effects, if incorrect measurements and uncertainties in the mode tracking procedure can be dismissed.
The results for 75 % and 100 % fill level indicate that the observed frequency shift is smaller than expected if the entire fluid mass contributed to the modal response, while the results for 50 %, which is almost $\eta_m = 1$ are consistent with a pure added mass interpretation for the tracked resonance frequency. However, this does not directly explain the pronounced resonance amplitudes observed at 50 % fill level, as these amplitudes may indicate additional effects.

Table 1 – Eigenfrequency prediction and effective modal fluid mass participation factor

Fill-Level (%)	**0 %**	**25 %**	**50 %**	**75 %**	**100 %**
Simulation (Hz)	336.57	274.81	237.99	212.87	194.32
Sensor 4 (Hz)	337.60	296.30	238.80	223.60	214.98
$f_{\mathrm{Prediction}}(\alpha)$	337	275.16	238.29	213.13	194.57
η_m	/	1.132	0.992	0.848	0.729

Figure 8 compares the experimental results with the two simplified simulation approaches. The solid lines with circular markers represent the simulation model based on density variation, while the dashed lines with square markers show the results obtained using the distributed added-mass approach. The experimental results are shown as dotted lines with triangular markers. The results from sensor position 2 were omitted from the graph because they were not representative for the investigated range of interest.
The fill-level sensitivity was evaluated by tracking selected resonance frequencies over all investigated fill states. The numerical models serve as reference trends for the expected mass loading behavior, while the experimental sensor data indicate the measured fill-level dependent frequency shifts. As shown in Figure 8, the experimental results generally follow the simulated trends and begin

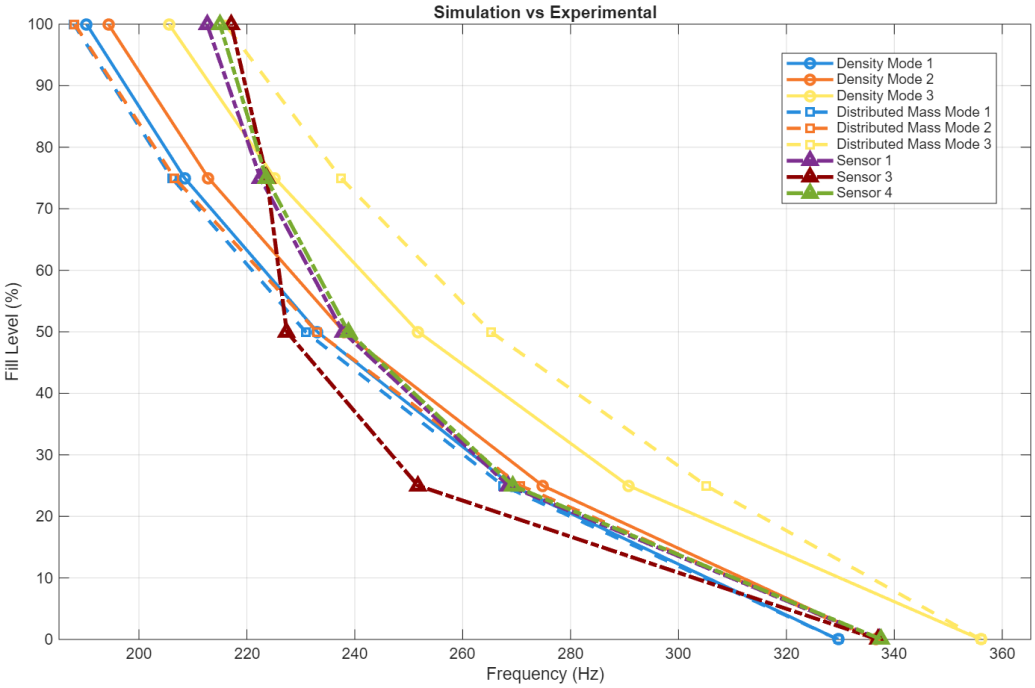


Figure 8 – Comparison of simulation to experimental results

to diverge more noticeably at higher fill levels. In particular, the results from sensor positions 1 and 4 show very similar behavior and follow the same general pattern as the simulation results.
The relative change in natural frequency between 100 % and 75 % fill level is comparatively small, whereas the frequency shift becomes more pronounced as the fluid mass decreases. This behavior is consistent with the trends observed in both the simulations and the analytical added mass approximation. Sensor position 3, however, shows a different behavior in the intermediate fill-level range. The resonance frequencies at 75 % and 50 % fill level are particularly close to each other, resulting in an almost negligible relative frequency shift. Consequently, fill-level estimation based on this sensor position would be difficult in this range and is likely to be less reliable and less accurate.

5. Discussion and Limitations of the Proposed Approach

Several limitations and simplifications of the present study should be considered when interpreting the experimental and numerical results.

- The investigated tank system does not represent a fully realistic LH_2 storage configuration suitable for aircraft applications, since the used pressure vessel was neither vacuum-insulated nor designed for cryogenic operation
- Water was used as a substitute fluid instead of LH_2
- Consequently, important effects related to cryogenic temperatures, material behavior and fluid properties were not captured
- The investigated fill levels were limited to increments of $25\,\%$
- Temperature-dependent changes in material stiffness, damping, thermal stresses, and fluid properties were not considered, as all experiments were conducted under ambient laboratory conditions
- Possible influences of ambient acoustic noise and external vibrations from the laboratory environment were also not systematically quantified, because environmental disturbances may contribute to measurement uncertainty
- The influence of internal pressure variations caused by evaporation and boil-off processes of cryogenic fluids could not be investigated

Since pressure-induced stiffness changes may additionally influence the modal characteristics of thin-walled tanks, future investigations under cryogenic operating conditions are required to assess the combined effects of fill level and internal pressure variations.
Furthermore, while the $25\,\%$ increment resolution is sufficient for an initial proof-of-concept investigation, smaller fill-level steps and a larger experimental dataset would be required to evaluate the achievable measurement accuracy and sensitivity in more detail.

The experimental boundary conditions also introduce additional uncertainties. The tank suspension using elastic expanders only approximates free-free boundary conditions and may introduce nonlinear stiffness and damping effects. Similarly, the direct attachment of the electrodynamic shaker locally affects the structural mass and stiffness distribution of the system. However, since the shaker configuration remained unchanged throughout all measurements, its influence on the comparative analysis of relative frequency shifts is considered limited.

Another important aspect is the dependency of modal observability on sensor placement. Certain vibration modes may only be detectable at specific sensor locations, while nodal regions can significantly reduce the measured response amplitudes. Although multiple sensor positions were investigated, the experimental identification of all relevant modes cannot be guaranteed.
Finally, the transferability of the proposed approach to practical aerospace applications remains an open question. Real aircraft tank systems are subject to varying operational conditions, structural complexity, temperature gradients, and dynamic flight maneuvers, all of which may influence the modal characteristics of the system. Further investigations under more representative operating conditions are therefore required to evaluate the practical applicability of modal-based fill-level estimation in aviation environments.

6. Conclusion and Outlook

The feasibility of modal-based fill-level estimation for cryogenic propellant tank applications using a combined experimental and numerical approach was investigated. The main objective was not the exact determination of the absolute eigenfrequencies of the investigated tank, but the identification of frequency shifts caused by changes in fluid mass. Experimental measurements were conducted on a suspended steel pressure vessel at five fill levels and four sensor positions, while simplified finite element models were used to estimate the expected mass-loading effect.

The experimental results confirm that selected resonance frequencies exhibit clear fill-level-dependent shifts and can therefore serve as indirect indicators of the contained fluid mass. However, the main finding is not the frequency shift itself, but the mode- and sensor-position-dependent suitability for fill-level estimation. While some resonances show distinct and reproducible trends over all investigated fill levels, others exhibit weak, irregular, or sensor-position-dependent behavior. This demonstrates that practical modal-based gauging cannot rely on arbitrary resonance peaks, but requires robust mode selection, sufficient modal observability, and reliable mode tracking.

The comparison between experiment and simulation shows that simplified added-mass models are suitable as a first-order reference for estimating the general frequency reduction of selected structural modes. However, the increasing deviations between measured and predicted resonance frequencies demonstrate that fill-level-dependent modal behavior cannot be fully reduced to a global mass-loading effect. This is particularly relevant for the transfer of modal gauging from established propellant-gauging applications toward aircraft-related cryogenic tank systems, where structural dynamics, sensor placement, and fluid-induced effects become critical design parameters.
The results therefore extend the state of the art by showing not only that resonance frequencies shift with fill level, but also that the suitability of individual modes must be critically assessed. Modes that follow the added-mass trend can be used for robust fill-level estimation, whereas resonances with amplified or irregular behavior indicate fluid-loaded structural modes or weakly coupled fluid-structure effects. Consequently, practical modal-based gauging systems should rely on selected, trackable

modes and require more detailed acoustic-fluid or coupled fluid-structure-interaction models for resonances that cannot be described by mass loading alone.

Overall, the results do not establish modal gauging as a new measurement principle, but demonstrate its application-oriented potential for aircraft-related cryogenic tank systems under simplified laboratory conditions. The main contribution of this study is the combined experimental and numerical assessment of fill-level-dependent frequency shifts, showing that selected, sensor-observable structural modes can be used for fill-level estimation, while other resonances require a more detailed treatment of fluid-induced effects. This highlights mode selection, sensor placement, and model fidelity as key requirements for transferring modal-based gauging toward LH_2 aircraft tank applications. Additionally, since the method can be implemented using externally mounted sensors, it avoids tank penetration and therefore does not introduce additional thermal bridges or direct heat input into the cryogenic storage system. This is particularly relevant for aircraft applications, where maintainability, structural integrity, and thermal efficiency are critical design aspects.

Nevertheless, further work is required before the approach can be considered applicable to aerospace fuel gauging. The present study was limited to water as a substitute fluid, a non-vacuum-insulated laboratory tank, coarse fill-level increments of 25 %, and simplified boundary conditions. Based on the observed mode-dependent sensitivity and sensor-position dependency, future work should focus on robust mode selection, mode tracking, and optimal sensor placement using smaller fill-level increments and repeated measurements. In addition, the transferability to aircraft-relevant cryogenic tanks must be investigated, particularly for double-walled and vacuum-insulated LH2 architectures, where externally mounted sensors may primarily capture the response of the outer shell rather than the inner vessel in contact with the liquid. Future studies should therefore also consider the structural coupling between inner and outer tank walls, insulation and support elements, cryogenic temperature effects, and dynamic operating conditions including acceleration-induced fluid motion, as well as susceptibility to sloshing should be assessed experimentally, for example using a Stewart Platform.

Further numerical work should include a more representative comparison between water and LH_2, in particular with respect to density and fluid-property effects. Moreover, acoustic-fluid modeling, sloshing effects, and fully coupled fluid-structure interaction should be investigated in more detail. The influence of internal pressure variations caused by evaporation and boil-off processes should also be considered, since pressure-induced stiffness changes may affect the modal response. Finally, practical implementation aspects need to be addressed, including whether ambient aircraft vibrations are sufficient for passive modal excitation, whether the method remains applicable for vacuum-insulated tank systems, and how the results change under fixed or aircraft-like mounting conditions.

7. Acknowledgement

This work was supported by the Austrian Federal Ministry for Climate Action, Environment, Energy, Mobility, Innovation and Technology (BMK) under the program Take Off via the project CroCo (Nr. FO999927749).

8. Contact Author Email Address

Mailto: simon.pfeifer@fh-joanneum.at

9. Copyright Statement

The authors confirm that they, and/or their company or organization, hold copyright on all of the original material included in this paper. The authors also confirm that they have obtained permission, from the copyright holder of any third party material included in this paper, to publish it as part of their paper. The authors confirm that they give permission, or have obtained permission from the copyright holder of this paper, for the publication and distribution of this paper as part of the ICAS proceedings or as individual off-prints from the proceedings.

References

[1] Saurav Tiwari, Michael J. Pekris, and John J. Doherty. A review of liquid hydrogen aircraft and propulsion technologies. *International Journal of Hydrogen Energy*, 57:1174–1196, 2024.

[2] ES Van der Sman, B Peerlings, J Kos, R Lieshout, and T Boonekamp. Destination 2050. *Netherlands Aerospace Centre NLR*, 2020.

[3] Stefan Kazula, Stefanie de Graaf, and Lars Enghardt. Review of fuel cell technologies and evaluation of their potential and challenges for electrified propulsion systems in commercial aviation. 2023.

[4] Pratikash P. Panda and Ethan S. Hecht. Ignition and flame characteristics of cryogenic hydrogen releases. *International Journal of Hydrogen Energy*, 42(1):775–785, January 2017.

[5] Alberto Boretti. Towards hydrogen gas turbine engines aviation: A review of production, infrastructure, storage, aircraft design and combustion technologies. *International Journal of Hydrogen Energy*, 2024.

[6] Wafa Suwaileh, Yusuf Bicer, Sara Al Hail, Saima Farooq, Rozan Mohamad Yunus, Nurul Nabila Rosman, and Imran Karajagi. Exploring hydrogen fuel as a sustainable solution for zero-emission aviation: Production, storage, and engine adaptation challenges. *International Journal of Hydrogen Energy*, 121:304–325, April 2025.

[7] Mehdi Soleymani, Vahid Mostafavi, Marie Hebert, Sousso Kelouwani, and Loïc Boulon. Hydrogen propulsion systems for aircraft, a review on recent advances and ongoing challenges. *International Journal of Hydrogen Energy*, 91:137–171, November 2024.

[8] Lawrence G. Edwards and Mark Haberbusch. Temperature and pressure effects on capacitance probe cryogenic liquid level measurement accuracy. Albuquerque, NM, September 1993. NTRS Author Affiliations: Analex Corp., Ohio Aerospace Inst. NTRS Report/Patent Number: NASA-CR-190763 NTRS Document ID: 19940012048 NTRS Research Center: Legacy CDMS (CDMS).

[9] K. Kochan, V. Weinig, O. Burkhardt, and J. Unteutsch. Modellbasierte Entwicklung kapazitiver Füllmengenmesssysteme für Flüssigwasserstofftanks in Flugzeugen. page 11 pages, October 2024. Artwork Size: 11 pages Medium: application/pdf Publisher: Deutsche Gesellschaft für Luft- und Raumfahrt - Lilienthal-Oberth e.V. Version Number: 1.0.

[10] Subodh K. Mital, John Z. Gyekenyesi, Steven M. Arnold, Roy M. Sullivan, Jane M. Manderscheid, and Pappu L. N. Murthy. Review of Current State of the Art and Key Design Issues With Potential Solutions for Liquid Hydrogen Cryogenic Storage Tank Structures for Aircraft Applications. Technical Report E-15621, October 2006. NTRS Author Affiliations: Toledo Univ., N and R Engineering, NASA Glenn Research Center NTRS Document ID: 20060056194 NTRS Research Center: Glenn Research Center (GRC).

[11] Michael Kotzem, Sebastian Wöhler, Tim Burschyk, Christian Hesse, and Sven Hellbrück. CONCEPTUAL AIRCRAFT DESIGN OF A RESEARCH BASELINE WITH DIRECT LIQUID HYDROGEN COMBUSTION.

[12] Marian-Cristian Staicu, Nicoleta Lucica Bogatu, Viorica Ghisman, and Daniela Laura Buruiana. Challenges and Innovations in Liquefied Gases and Cryogenic Tanks: A Comprehensive Review. *Technologies*, 14(1):19, January 2026. Publisher: Multidisciplinary Digital Publishing Institute.

[13] Abhay Singh Gour, Pankaj Sagar, and R. Karunanithi. Investigation of cryogenic level sensors for LN 2 and LOX. *Cryogenics*, 84:76–80, June 2017.

[14] Paula J Dempsey and Richard H Fabik. USING SILICON DIODES FOR DETECTING THE LIQUID-VAPOR INTERFACE IN HYDROGEN. *38th International Instrumentation Symposium*, April 1992.

[15] SAE Media Group. Cryogenic Liquid Level Sensor Apparatus and Method, September 2016.

[16] J. Talpe, G. Stolovitzky, and V. Bekeris. Cryogenic thermometry and level detection with common diodes. *Cryogenics*, 27(12):693–695, December 1987.

[17] Jianchun Yang, Zining Zhao, Xiaobing Li, Xinke Li, and Wenjing Yang. A cryogenic liquid level sensor based on EFPI-FBG. *Measurement*, 257:118842, January 2026.

[18] Kevin M. Crosby, Nehemiah J. Williams, Rudolph J. Werlink, and Eric A. Hurlbert. Modal Propellant Gauging: High-resolution and non-invasive gauging of both settled and unsettled liquids in reduced gravity. *Acta astronautica*, 159:499–507, June 2019.

[19] Kevin M. Crosby, Rudy J. Werlink, and Eric A. Hurlbert. Liquid Propellant Mass Measurement in Microgravity. *Gravitational and Space Research*, 9(1):50–61, February 2021.

[20] Kevin Crosby, Eric A. Hurlbert, and Rudolph J. Werlink. Liquid mass gauging during propellant transfer in microgravity. *Acta Astronautica*, 220:283–296, July 2024.

[21] Eytan J. Adler and Joaquim R.R.A. Martins. Hydrogen-powered aircraft: Fundamental concepts, key technologies, and environmental impacts. *Progress in Aerospace Sciences*, 141:100922, August 2023.

[22] D. J. Ewins. *Modal Testing: Theory, Practice and Application*. Research Studies Press, 2000.

[23] Daniel J. Inman. *Engineering Vibration*. Pearson, 2014.

[24] R.B. Davis. A simplified approach for predicting interaction between flexible structures and acoustic enclosures. *Journal of Fluids and Structures*, 70:276–294, April 2017.

[25] P. Moussou. A kinematic method for the computation of the natural modes of Fluid–Structure Interaction systems. *Journal of Fluids and Structures*, 20(5):643–658, July 2005.

[26] Kevin M. Crosby, Tessa Rundle, Kevin LeCaptain, and Rudy Werlink. Modal Propellant Gauging in Low Gravity. *SPACE Conferences and Exposition : AIAA SPACE 2016*, 2016:1–8, 2016.

[27] Arturo Gomez and Howard Smith. Liquid hydrogen fuel tanks for commercial aviation: Structural sizing and stress analysis. *Aerospace Science and Technology*, 95:105438, December 2019.

[28] G. Onorato, P. Proesmans, and M. F. M. Hoogreef. Assessment of hydrogen transport aircraft. *CEAS Aeronautical Journal*, 13(4):813–845, October 2022.

[29] J. Huete, D. Nalianda, and P. Pilidis. Impact of tank gravimetric efficiency on propulsion system integration for a first-generation hydrogen civil airliner. *The Aeronautical Journal*, 126:1–9, June 2022.

[30] Daniel Raymer. *Aircraft Design: A Conceptual Approach, Sixth Edition*. September 2018.

[31] Jon Huete and Pericles Pilidis. Parametric study on tank integration for hydrogen civil aviation propulsion. *i n t e r n a t i o n a l journal o f hydrogen energy 4 6*, 2021.